

Updated database for L x-ray production by protons and extraction of L -subshell ionization cross sections from only L_γ and $L_\alpha + L_\beta$ cross sections

Gregory Lapicki^{a*} and Javier Miranda^b

Database from pre-1995 compilations of L x-ray production and ionization by protons is enlarged by 53% with the present update. Semiempirical formulas for L_γ and $L_{\alpha\beta}$ are developed and used to extract L_1 , L_2 , and L_3 subshell ionization cross sections. The extracted ionization cross sections are shown for a sample of elements and compared with the database ionization cross sections in gold. Copyright © 2011 John Wiley & Sons, Ltd.

Previous Database and its Update

The database used for this study originates with the data compiled in in Refs [1–3]. With additional references [4–8] that were not cited in these compilations and the subsequently published data,^[9–32] a total of 29 papers was found, including several that presented the results only in graphical form.^[4–8] The graphs from these papers were digitized and the values extracted in tabular form, although a higher uncertainty in these values should be expected. Figure 1 compares the number of the reported L -subshell ionization and the individual x-ray line cross sections as previously compiled and currently updated. With all these new data, the cumulative database has 2766 sets of cross sections from which cross sections for L_1 , L_2 , and L_3 subshell ionization by protons in the atomic number range of targets $39 \leq Z_2 \leq 92$ could be potentially extracted. The complete database comprises three classes of data: 36% or 992 sets of data with L_ℓ , L_α , L_β , and L_γ with L_γ sublines ($L_{\gamma 1}$, $L_{\gamma 23}$, $L_{\gamma 44}$); 28% or 781 sets of data with L_ℓ , L_α , L_β , and L_γ without those L_γ sublines; and 36% or 993 sets of data with L_1 , L_2 , and L_3 subshell ionization cross sections. Additionally, for a complete collection of $\{L_\ell, L_\alpha, L_\beta, L_\gamma\}$, those L_1 , L_2 , and L_3 ionization cross sections were converted to x-ray line cross sections with the atomic parameters used in the article in which they were reported.

Figure 2 displays the number of available experimental x-ray production (XRP) and ionization data sets from 1972 up to 2009, as given in Refs [1–3] and the present compilation. While a cumulative rate of increase in that number of about 80 such sets per year in the 1972–1994 period has slowed to about 40 in this millennium, the present update exceeds the previous compilations by a 53%. A total of 1773 $\{L_\alpha, L_\beta, L_\gamma\}$ XRP and of 993 $\{L_1, L_2, L_3\}$ ionization cross sections reconverted to the XRP will be employed to extract L -subshell ionization cross sections.

Extraction of L_1 , L_2 , and L_3 Subshell Ionization cross sections: Traditional and Present Methods

Cohen^[33] reviewed four traditional techniques for the extraction of L -subshell ionization cross sections from XRP data: (1) solving

three equations with $\{L_\alpha, L_\beta, L_\gamma\}$ for three unknowns $\{L_1, L_2, L_3\}$, (2) solving three equations with $\{L_\alpha, L_{\gamma 1}, L_\gamma\}$ for three unknowns $\{L_1, L_2, L_3\}$, (3) based on $\{L_\alpha, L_{\gamma 6}, L_{\gamma 236}\}$ the Datz technique^[4] that to get L_1 removes $L_{\gamma 6}$ due to L_2 from $L_{\gamma 236}$, and (4) Cohen's fine tuning on the first two techniques with an adjustment of the branching ratios until these two techniques yielded the same L_1 . As noted in Ref [34], 'the contributions from L_1 and L_2 to L_β and L_γ are comparable. Therefore, the L_1 and L_2 cross sections obtained by this procedure are rather sensitive to the accurate L_β and L_γ intensities as well as branching ratios of the L_1 and L_2 subshells into these line groups.' The 'rather sensitive' in this note is an understatement. The inverse of the matrix that yields the measured $\{L_\alpha, L_\beta, L_\gamma\}$ in terms to-be-extracted $\{L_1, L_2, L_3\}$ is often ill-defined; as solutions to a set of three equations, the extracted cross sections are highly unreliable and sometimes even negative.

The inadequacy or outright failure of several of these techniques stems from two major obstacles: for low- Z_2 elements the x-ray peaks are impossible or extremely difficult to resolve due to their considerable overlap and while with increasing Z_2 , these difficulties subside, a slightly erroneous background subtraction may generate false assignments of x-ray counts to $\{L_\alpha, L_\beta, L_\gamma\}$ or $\{L_\alpha, L_{\gamma 1}, L_\gamma\}$ lines.

To circumvent these obstacles, due to limited resolution compounded by background subtraction uncertainties, an extraction of $\{L_1, L_2, L_3\}$ cross sections should be grounded on a method that does not require any resolution between L_α and L_β peaks, nor does it necessitate a surgical distinction between the x-ray lines that make up the L_γ peak. In fact, since L_γ originates from L_1 and L_2 only while both L_α and L_β involve all three subshells, it is natural to anchor an extraction of $\{L_1, L_2, L_3\}$ cross sections on L_γ and a

* Correspondence to: Gregory Lapicki, Department of Physics, East Carolina University, Greenville, NC 27858, USA. E-mail: lapicki@physicist.net

a Department of Physics, East Carolina University, Greenville, NC 27858, USA

b Instituto de Física, Universidad Nacional Autónoma de México, A.P. 20-364, México, D.F. 01000, Mexico

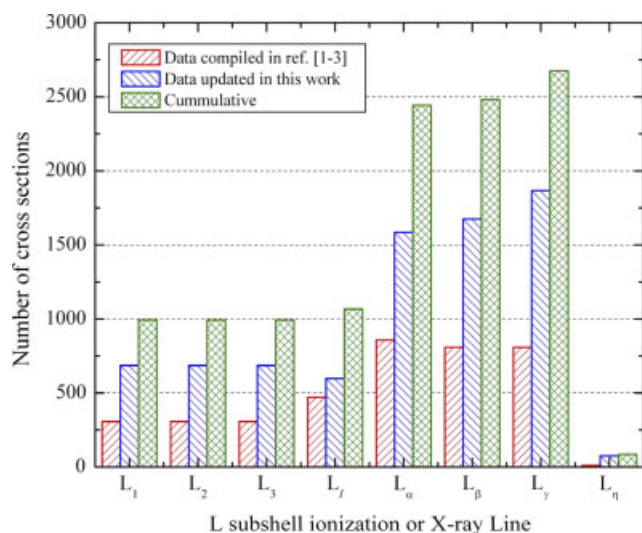


Figure 1. Number of L-subshell ionization and the individual x-ray line cross sections as previously compiled^[1–3] and currently updated.^[4–32]

combined $L_{\alpha\beta} \equiv L_{\alpha} + L_{\beta}$. Furthermore, such a procedure imposes less stringent conditions on the accuracy of atomic parameters – a separate conversion of (L_1, L_2, L_3) to L_{α} and L_{β} requires six numbers, while $L_{\alpha\beta}$ is based on just three numbers stemming from a given set of atomic parameters. Atomic parameters were taken as recommended in Ref [35] for branching ratios and Campbell for fluorescence and Coster–Kronig yields.^[36,37]

Instead of solving an overdetermined set of two equations for L_{γ} and $L_{\alpha\beta}$ with three (L_1, L_2, L_3) unknowns, a search is made for a pair of positive $(L_1/L, L_2/L)$ ratios that, with $L_3/L \equiv 1 - L_1/L - L_2/L$, minimizes

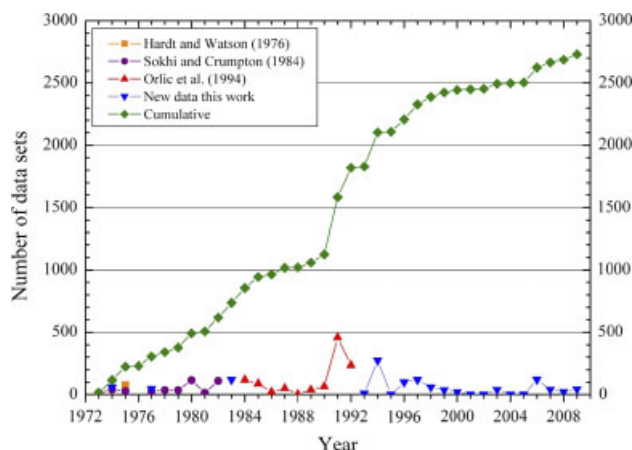


Figure 2. Histogram of experimental XRP and ionization data sets^[1–3] and the present compilation^[4–32] up to 2009.

$$\left(1 - \frac{\sigma_{L\gamma}^{\text{empirical}}}{\sigma_{L\gamma}^{\text{calculated}}}\right)^2 + \left(1 - \frac{\sigma_{L\alpha\beta}^{\text{empirical}}}{\sigma_{L\alpha\beta}^{\text{calculated}}}\right)^2 \quad (1)$$

This method did not yield satisfactory results, when for a given element, raw data were used for $\sigma_{L\gamma}^{\text{empirical}}$ and $\sigma_{L\alpha\beta}^{\text{empirical}}$. Therefore, semiempirical formulas are developed for $\sigma_{L\gamma}$ and $\sigma_{L\alpha\beta}$.

Extraction of $L_1, L_2,$ and L_3 Subshell Ionization cross sections with Semiempirical Formulas for $L_{\alpha\beta}$ and L_{γ} cross sections

Figure 3(a) displays empirical cross sections, $\sigma_{L\alpha\beta}^{\text{empirical}}$, plotted versus x defined as the proton velocity v_1 scaled by the electron

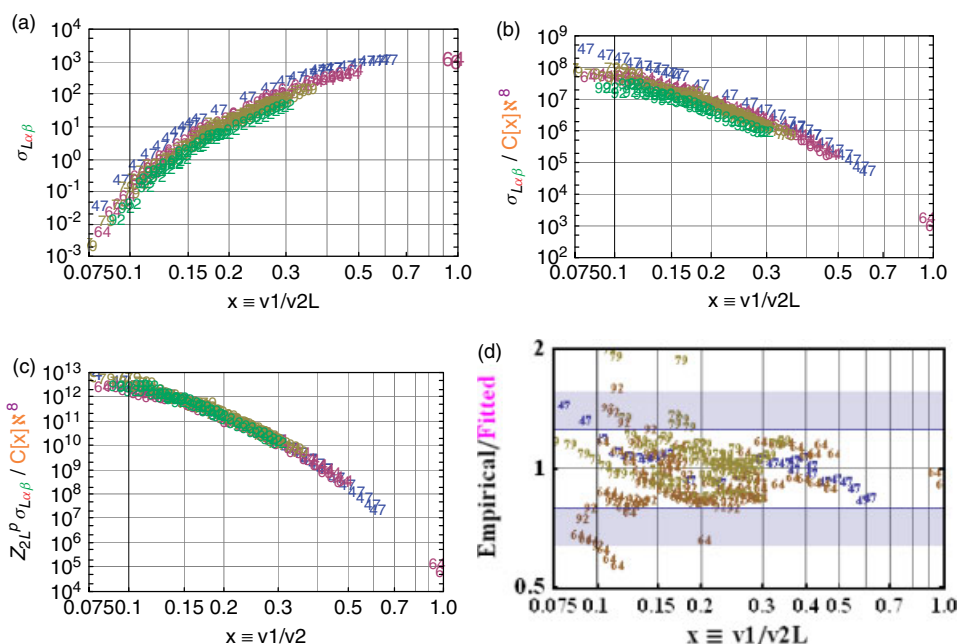


Figure 3. (a) Empirical cross sections, $\sigma_{L\alpha\beta}^{\text{empirical}}$, plotted versus x defined as the proton velocity v_1 scaled by the electron orbital velocity $v_{2L} = Z_{2L}/2$, with $Z_{2L} = Z_2 - 4.15$, for $47 \leq Z_2 \leq 92$ elements; (b) $\sigma_{L\alpha\beta}^{\text{empirical}}$ scaled by $C[x]x^8$ dictated by L_1 behavior in the low- x limit according to Ref. [38] where $C[x]$ of Eqn (2) is a Coulomb deflection factor; (c) $\sigma_{L\alpha\beta}^{\text{empirical}}$, scaled by $C[x]x^8$ and multiplied by Z_{2L}^p where $p = 3 - x^{1/2} - x$ in pursuit of a universal curve fitted with $\sigma_{L\alpha\beta}^{\text{semiempirical}}$ of Eqn (3); (d) ratios of empirical cross sections to results of the fitted semiempirical formula as given by Eqn (3).

orbital velocity $v_{2L} = Z_{2L}/2$ for $47 \leq Z_2 \leq 92$ elements, with $Z_{2L} = Z_2 - 4.15$. At $x < 0.1$, the empirical cross sections fall too steeply to be efficiently fitted to a power of x . This precipitous drop-off results from an essentially exponential decrease in the ionization of L -subshells due to the Coulomb deflection of the proton by the target nucleus. With the L_1 subshell dominating over other subshells in the low- x limit, according to Ref [38] the Coulomb deflection is given by

$$C[x] = 9 \exp(-\pi dq) / (9 + \pi dq), \quad (2)$$

where in terms of x , the symmetrized^[39] $\pi dq = (0.11/x)^3 2 / [1 + (1 - 1/1823x^2)^{1/2}] / [1 - (1/1823x^2)^{1/2}]$.

Based on L_1 proportionality to x^8 in the plane-wave Born approximation (PWBA) at the low x limit,^[38] the $\sigma_{L\alpha\beta}^{\text{empirical}}$ are further scaled by x^8 ; Fig. 3(b) shows $\sigma_{L\alpha\beta}^{\text{empirical}}$ divided by $C[x]x^8$. There is still a dependence on Z_{2L} . In the low- x limit, the PWBA cross sections for the L_1 subshell is inversely proportional to Z_{2L}^4 and θ_{2L}^9 , where θ_{2L} is the observed L -shell-binding energy divided by its screened hydrogenic $Z_{2L}^2/8$ value. In the $39 \leq Z_2 \leq 92$ and in the range of x common to the lightest and heaviest elements, θ_{2L}^9 is inversely proportional to Z_{2L}^2 . Thus ionization cross sections multiplied by fluorescence yields, which are proportional to Z_{2L}^3 , leads to $\sigma_{L\alpha\beta}$ being inversely proportional to Z_{2L}^3 in the low- x regime. As $x \rightarrow 1$, however, $\sigma_{L\alpha\beta}$ becomes inversely proportional to Z_{2L} . Hence, bringing scaled cross sections to a universal curve in x – as illustrated in Fig. 3(c) – $\sigma_{L\alpha\beta}^{\text{empirical}} / C[x]x^8$ are multiplied by Z_{2L}^p where $p = 3 - x^{1/2} - x$. This curve is fitted by the following semiempirical formula:

$$\sigma_{L\alpha\beta}^{\text{semiempirical}} = 7.1 \cdot 10^{13} \text{ barn} \frac{C[x]x^8 \exp(-35x + 24x^2 - 10x^3)}{Z_{2L}^{(3-x^{1/2}-x)}} \quad (3)$$

Figure 3(d) shows ratios of empirical cross sections to results of the fitted formula as given by Eqn (3). Half of all compiled data lie within 10% of $\sigma_{L\alpha\beta}^{\text{semiempirical}}$; 87% are within 25% and 94% are within 50% of this fit.

Figure 4 displays ratios of the compiled L_Y cross sections, $\sigma_{LY}^{\text{empirical}}$ to $\sigma_{L\alpha\beta}^{\text{semiempirical}}$ of Eqn (3). In Fig. 4(a), all ratios are

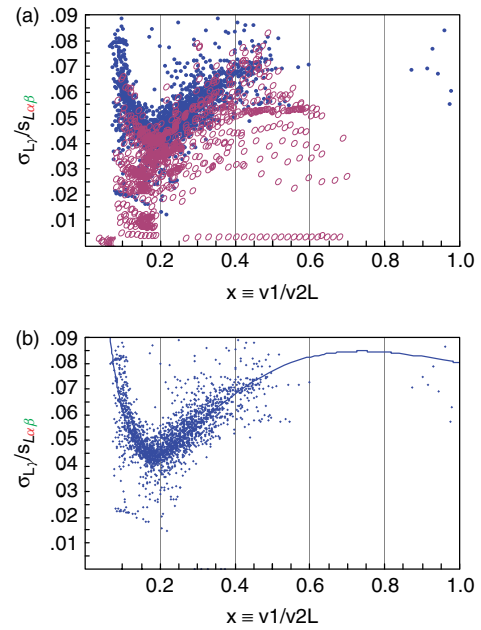


Figure 4. Ratios of the compiled L_Y cross sections, $\sigma_{LY}^{\text{empirical}}$, to $\sigma_{L\alpha\beta}^{\text{semiempirical}}$ of Eqn (3). (a) All ratios are shown as solid symbols for $57 < Z_2 \leq 92$ targets and open symbols for $39 \leq Z_2 \leq 57$; (b) ratios for $57 < Z_2 \leq 92$ and a curve to fit them as given in Eqn (4).

shown as solid symbols for $57 < Z_2 \leq 92$ targets and open symbols for $39 \leq Z_2 \leq 57$; Fig. 4(b) shows these ratios for $57 < Z_2 \leq 92$ and a curve to fit them as follows:

$$\left(\frac{\sigma_{LY}}{\sigma_{L\alpha\beta}} \right)^{\text{semiempirical}} = 0.046 \left[1 + \frac{(\log(x) + 1.72)^2}{(1 + x^2)^2} \right] \quad (4)$$

In Fig. 5, these ratios are shown for selected elements with an extension of Eqn (4) to

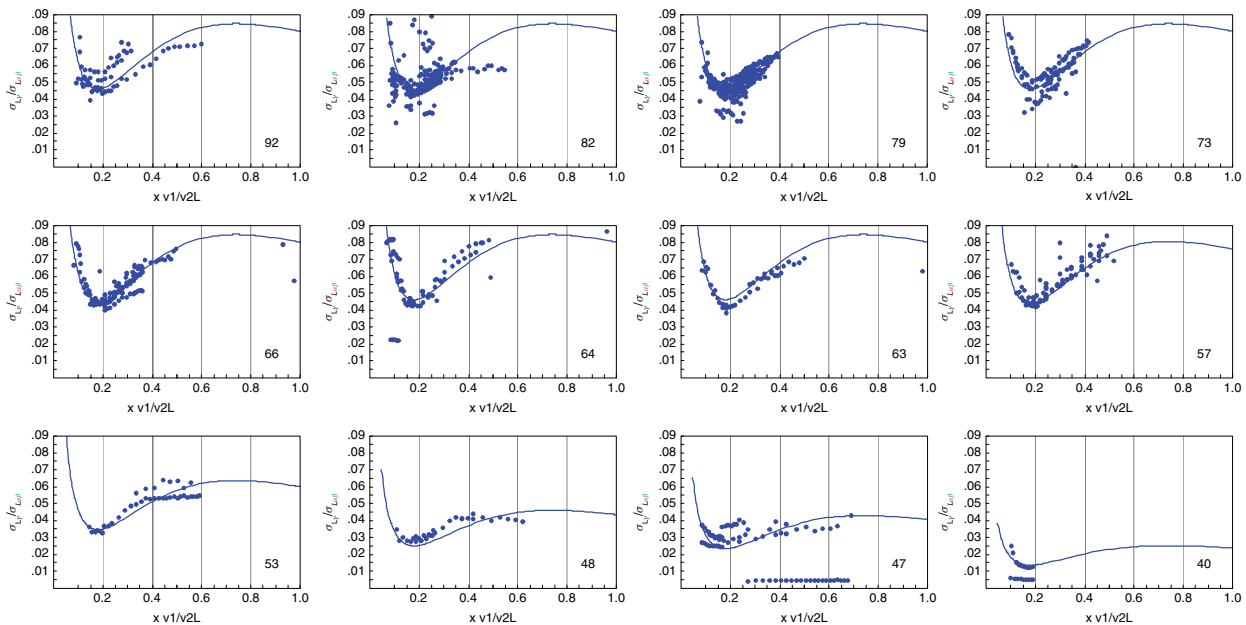


Figure 5. $(\sigma_{LY}/\sigma_{L\alpha\beta})^{\text{empirical}}$ and $(\sigma_{LY}/\sigma_{L\alpha\beta})^{\text{semiempirical}}$ [curves according to Eqns (4) and (5)] for selected elements.

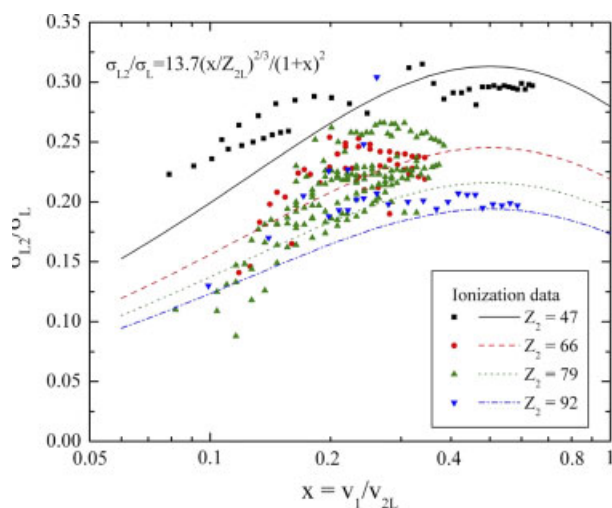


Figure 6. Ratios of L_2/L ionization cross sections according to the database (symbols) and Eqn (6) (curves).

$$\left(\frac{\sigma_{L\gamma}}{\sigma_{L\alpha\beta}}\right)^{\text{semiempirical}} = \left(\frac{Z_{2L}}{150}\right)^3 \left[1 + \frac{(\log(x) + 1.72)^2}{(1+x)^2}\right] \quad (5)$$

for $39 \leq Z_2 \leq 57$ elements.

Extraction of L_1 , L_2 , and L_3 Subshell Ionization cross sections with Semiempirical Formulas for $L_{\alpha\beta}$ and L_{γ} cross sections and a Constraint on L_2/L Ratios

The replacement of raw empirical cross sections with these semiempirical formulas still did not produce good results. Hence,

the least-square fit in Eqn (1) was performed with a constraint that L_2/L ratios be varied within the $[-0.01, +0.01]$ interval around

$$L_2/L = 13.7(x/Z_{2L})^{2/3} / (1+x)^2 \quad (6)$$

which was constructed to mimic the ratios obtained from the database for L -subshell ionization (Fig. 6).

Figure 7 shows the L -subshell ionization cross sections in silver, dysprosium, gold, and uranium that were extracted using semiempirical formulas of Eqns (3)–(5) with the constraint of Eqn (6) in the method presented above. The extracted ^{79}Au cross sections are compared with all published ionization data in Fig. 8(a) and with the ionization data from a single reference [4] in Fig. 8(b). There is an excellent agreement between the extracted L_2 and L_3 cross sections and the ionization database cross sections. For L_1 subshell, the considerable scatter of all reported ionization cross sections precludes definitive judgment on the merit the cross sections extracted according to this work. Yet, there is a perfect agreement once compared with the ionization data of Ref [4] It might be that the Datz technique is just as effective as the method of extraction of L -subshell ionization cross sections from L_{γ} and $L_{\alpha\beta}$ proposed in this work or it could be that this agreement is purely accidental.

Conclusions

Going beyond the existing collections of cross sections for L -shell XRP and ionization by protons, an enlarged compilation of such data served as an input for semiempirical formulas for $L_{\alpha\beta}$ and L_{γ} XRP cross sections. A preliminary test of extraction of the L -subshell ionization cross sections in gold from these semiempirical formulas suggests an efficient method for further analysis of the

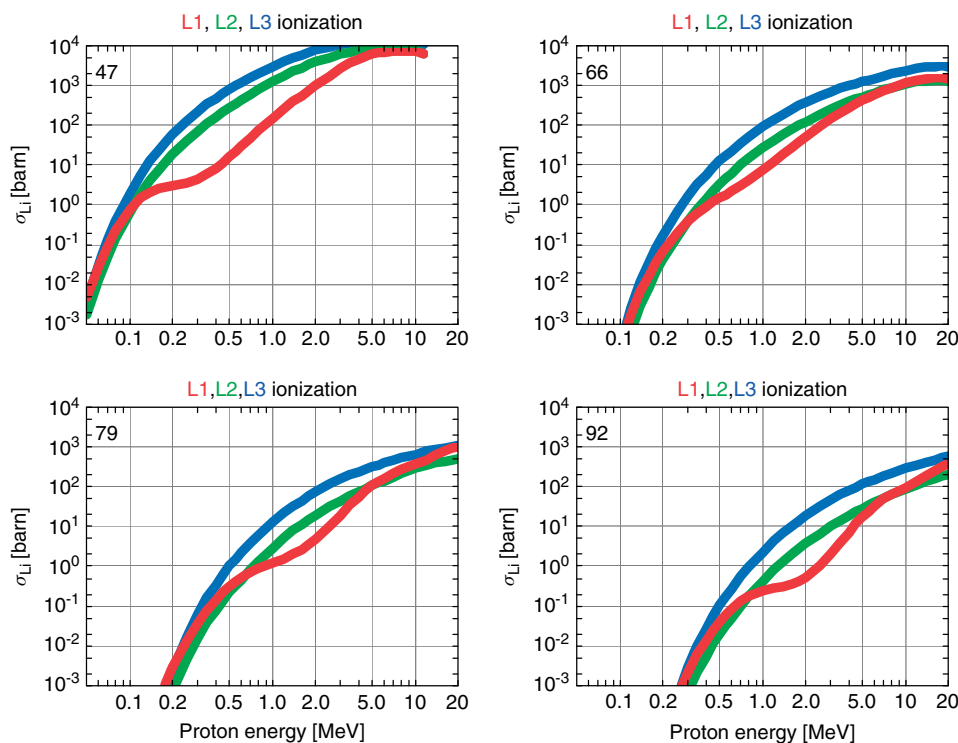


Figure 7. Extracted L_1 , L_2 , and L_3 ionization cross sections in ^{47}Ag , ^{66}Dy , ^{79}Au , and ^{92}U by protons.

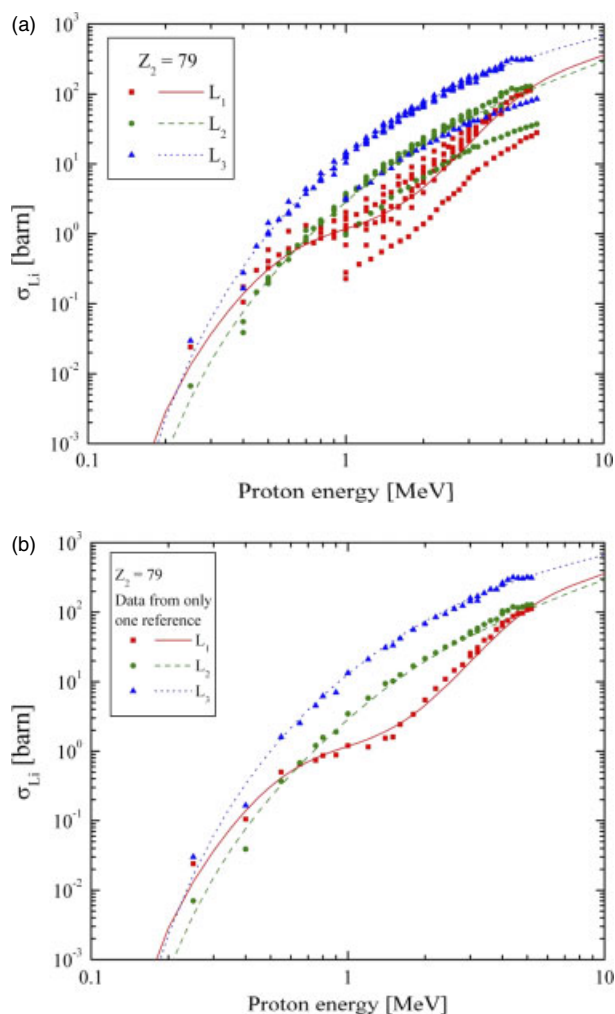


Figure 8. Extracted L_1 , L_2 , and L_3 ionization cross sections in ^{79}Au by protons (curves) compared with ionization cross sections from all references in the database in (a) and with the ionization cross sections from Ref [4] in (b).

L -subshell ionization vis-à-vis theoretical predictions and in applications such as an input ingredient for PIXE codes. As the further update of the present compilation continues, the method that is outlined here for the extraction of L -subshell ionization cross sections will be comprehensively examined for its reliability in a broad range of target elements.

References

[1] T. L. Hardt, R. L. Watson, *At. Data Nucl. Data Tables* **1976**, 17, 107.
 [2] R. S. Sokhi, D. Crumpton, *At. Data Nucl. Data Tables* **1984**, 30, 49.
 [3] I. Orlic, C. H. Sow, S. M. Tang, *At. Data Nucl. Data Tables* **1994**, 56, 169.

[4] S. Datz, J. L. Duggan, L. C. Feldman, E. Laegsgaard, J. U. Andersen, *Phys. Rev. A* **1974**, 9, 192.
 [5] C. N. Chang, J. F. Morgan, S. L. Blatt, *Phys. Rev. A* **1975**, 11, 607.
 [6] T. K. Li, D. L. Clark, G. W. Greenlees, *Phys. Rev. A* **1976**, 14, 2016.
 [7] J. R. Chen, *Phys. Rev. A* **1977**, 15, 487.
 [8] E. Rosato, *Phys. Rev. A* **1983**, 28, 2759.
 [9] Z. Szökefalvi-Nagy, I. Demeter, L. H. Quynh, *Nucl. Instr. Meth. B* **1993**, 75, 54.
 [10] C. H. Sow, I. Orlic, T. Osipowicz, S. M. Tang, *Nucl. Instr. Meth. B* **1994**, 85, 133.
 [11] L. Rodríguez-Fernández, J. Miranda, A. Oliver, *Nucl. Instr. Meth. B* **1994**, 85, 150.
 [12] S. Fazinic, I. Bogdanovic, M. Jaksic, I. Orlic, V. Valkovic, *Nucl. Instr. Meth. B* **1994**, 94, 363.
 [13] H. C. Padhi, C. R. Bhuinya, B. B. Dhal, S. Misra, *J. Phys. B* **1994**, 27, 1105.
 [14] Y. C. Yu, E. K. Lin, C. W. Wang, P. J. Tsai, C. H. Chang, *J. Phys. B* **1994**, 27, 3967.
 [15] S. Bogdanovic, M. Fazinic *J. Phys. B* **1996**, 29, 2021.
 [16] I. B. Vodopyanov, V. V. Pashuk, M. V. Stabnikov, *J. Phys. B* **1996**, 29, 2543.
 [17] E. Perillo, G. Spadaccini, M. Vigilante, P. Cuzzocrea, N. De Cesare, *Int. J. PIXE* **1996**, 6, 3.
 [18] I. Bogdanovic, S. Fazinic, M. Jaksic, I. Orlic, V. Valkovic, *Nucl. Instr. Meth. B* **1996**, 109, 47.
 [19] S. J. Cipolla, M. J. Dolezal, L. O. Casazza, *AIP Conf. Proc.* **1997**, 392, 113.
 [20] S. J. Cipolla, *AIP Conf. Proc.* **1997**, 392, 117.
 [21] A. Amirabadi, H. Afarideh, S. M. Haji-Saeid, F. Shokouhi, H. Peyrovan, *J. Phys. B* **1997**, 30, 863.
 [22] V. John Kennedy, A. Augusthy, K. M. Varier, P. Magudapathy, K. G. M. Nair, B. B. Dhal, H. C. Padhi, *Nucl. Instr. Meth. B* **1998**, 134, 165.
 [23] N. De Cesare, E. Perillo, G. Spadaccini, M. Vigilante, *Nucl. Instr. Meth. B* **1998**, 136, 189.
 [24] A. Balsamo, N. De Cesare, F. Murolo, E. Perillo, G. Spadaccini, M. Vigilante, *J. Phys. B* **1999**, 32, 5699.
 [25] M. Hajivaliei, S. Puri, M. L. Garg, D. Mehta, A. Kumar, S. K. Chamoli, D. K. Avasthi, A. Mandal, T. K. Nandi, K. P. Singh, N. Singh, I. M. Govil, *Nucl. Instr. Meth. B* **2000**, 160, 203.
 [26] S. J. Cipolla, *AIP Conf. Proc.* **2003**, 680, 15.
 [27] M. Goudarzi, F. Shokouhi, M. Lamehi-Rachti, P. Oliyai, *Nucl. Instr. Meth. B* **2006**, 247, 217.
 [28] S. Ouziane, A. Amokrane, I. Toumert, A. Nourredine, A. Pape, *Nucl. Instr. Meth. B* **2006**, 249, 73.
 [29] H. Mohan, A. K. Jain, *Nucl. Instr. Meth. B* **2008**, 266, 1203.
 [30] S. Ouziane, A. Amokrane, I. Toumert, *Nucl. Instr. Meth. B* **2008**, 266, 1209.
 [31] S. J. Cipolla, *AIP Conf. Proc.* **2009**, 1099, 180.
 [32] S. J. Cipolla, *J. Phys. B* **2009**, 42, 205201.
 [33] D. D. Cohen, *J. Phys. B* **1984**, 17, 3917.
 [34] W. Jitschin, R. Hippler, K. Fink, R. Schuch, H. O. Lutz, *J. Phys. B* **1983**, 16, 4405.
 [35] J. L. Campbell, J.-X. Wang, *At. Data Nucl. Data Tables* **1983**, 43, 281.
 [36] J. L. Campbell, *At. Data Nucl. Data Tables* **2003**, 85, 203.
 [37] J. L. Campbell, *At. Data Nucl. Data Tables* **2009**, 95, 115.
 [38] W. Brandt, G. Lapicki, *Phys. Rev. A* **1974**, 10, 474.
 [39] W. Brandt, G. Lapicki, *Phys. Rev. A* **1981**, 23, 1717.